Observation of ferrotoroidic domain pattern by linear and nonlinear optical effects

Sato Tatsuki [1], Sekine Daiki [2]

[1] Department of Advanced Materials Science, University of Tokyo

[2] Department of Physics, Tohoku University

0. About the authors

Sato Tatsuki specializes in the experimental study of the magnetoelectric coupling in transition metal compounds. In this research, he prepared a single crystal of $MnTiO_3$ and performed imaging study based on the linear optical effect.

Sekine Daiki specializes in the experimental study of the nonlinear optical measurements to multipole orders realized in nano- to meso-scale. In this research, he performed imaging study by using optical second harmonic generation.

1. Introduction

Antiferromagnets without magnetization are characterized by magnetic multipole degrees of freedom. Recently, electromagnetic responses in antiferromagnets, such as the anomalous Hall effects and the magnetoelectric effect, are explained in terms of corresponding magnetic multipoles [1,2]. Thus, manipulation of magnetic multipole degrees of freedom is inevitable to fully utilize such functionalities of antiferromagnets. Switching between two distinct magnetic states is usually achieved via the transient state with multidomain state where the two magnetic states coexist. Knowledge of magnetic multipole domain patterns would be helpful in future implementation of antiferromagnetic materials in devices.

Direct observation is one of the most major techniques to study domain patterns. Optical imaging of domain pattern is made possible by employing the appropriate optical effects. In contrast to magnetic-domain imaging in ferromagnets based on magnetic circular dichroism (MCD), domain imaging in antiferromagnets where MCD is absent is rather difficult. Among several currently developed imaging techniques in antiferromagnets [3], optical imaging techniques based on linear optical effects, such as magneto-optical Kerr effect and nonreciprocal optical effect, and those based on optical second harmonic generation (SHG), which is a nonlinear optical effect, are widely used to study multipole domain patterns in many materials.

Combination of several imaging techniques should provide us more information about domain patterns than imaging study based on a single imaging technique. Here, we employed both linear and nonlinear optical effects to investigate magnetic multipole domain patterns in an antiferromagnet. We focused on domain structures of the magnetic toroidal moment, which is the source of nonreciprocal phenomena. We performed two types of imaging experiments on a single sample to study the domain structure both at the surface and in the bulk of the sample.

2. Ferrotoroidic Antiferromagnet $MnTiO_3$

In this study, we focused on ferrotoroidic antiferromagnet $MnTiO_3$. $MnTiO_3$ crystallizes in the ilmenite

structure with the centrosymmetric point group -3. A buckled honeycomb layer of Mn^{2+} ions with $S = 5/2$ in the c plane is shown in Fig. 1(a). All Mn^{2+} ions are octahedrally coordinated by six oxygen ions. Below the Néel temperature $T_N = 65$ K, $MnTiO_3$ adopts easy-axis collinear antiferromagnetic ordering without doubling the unit cell. The magnetic symmetry is -3'. Magnetic unit cells are shown in Fig. 1(b). Antiferromagnetic order parameter is the staggered magnetization $\boldsymbol{L}$.

In the magnetic symmetry -3', the magnetic toroidal moment $\boldsymbol{T}$ is oriented along the c axis of the crystal. Two distinct states with magnetic moments in opposite directions are characterized by $\boldsymbol{L}$ in opposite directions [see Fig 1(b)]. Since the antiferromagnetic order parameter $\boldsymbol{L}$ and the toroidal moment $\boldsymbol{T}$ both behaves odd to the time reversal operation, the directions of $\boldsymbol{L}$ and $\boldsymbol{T}$ are in one-to-one correspondence as depicted in Fig. 1(b).

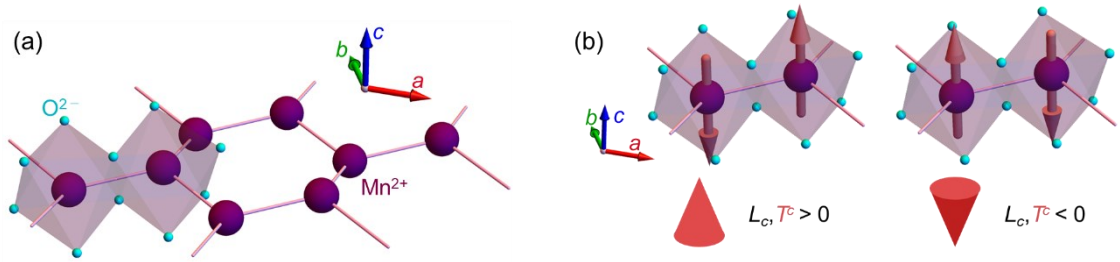

Figure 1: (a) Honeycomb structure in $MnTiO_3$. (b) Relation between staggered magnetization $\boldsymbol{L}$ and toroidal moment $\boldsymbol{T}$. Red cones depict directions of toroidal moments.

3. Methods

3.1 Ferrotoroidic domain imaging based on the linear optical effect

When unpolarized light propagates along the toroidal moment $\boldsymbol{T}$, absorption coefficients α depends on the configuration between the direction of the propagation vector $\boldsymbol{e_k}$ and $\boldsymbol{T}$ as

$$\alpha(\boldsymbol{e_k} \uparrow\uparrow \boldsymbol{T}) \neq \alpha(\boldsymbol{e_k} \uparrow\downarrow \boldsymbol{T}). \quad (1)$$

Equation (1) represents magnetochiral dichroism (MCHD). MCHD in $MnTiO_3$ is schematically illustrated in Fig. 2(a). Since the toroidal moment $\boldsymbol{T}$ is along the c axis in $MnTiO_3$, MCHD shows up as the directional dichroism for light propagating along the c axis when the direction of $\boldsymbol{T}$ is fixed. When the propagation direction $\boldsymbol{e_k}$ of light is fixed, the absorption coefficient α changes for the reversal of $\boldsymbol{T}$.

MCHD enables us to visualize ferrotoroidic domain patterns. When the prorogation direction of light $\boldsymbol{e_k}$ is fixed, two distinct states with $\boldsymbol{T}$ in opposite directions are distinguished by the difference in transmitted light intensity [see Eq. (1)]. Figure 2(b) shows experimental setup for MCHD-based imaging of ferrotoroidic domain pattern. Obtained patterns in the MCHD-based imaging in this transmission configuration represent the projection along the c axis of the original domain distribution in three dimensions. The imaging experiments were carried out at a wavelength $\lambda = 575$ nm where the prominent MCHD signal is observed [4].

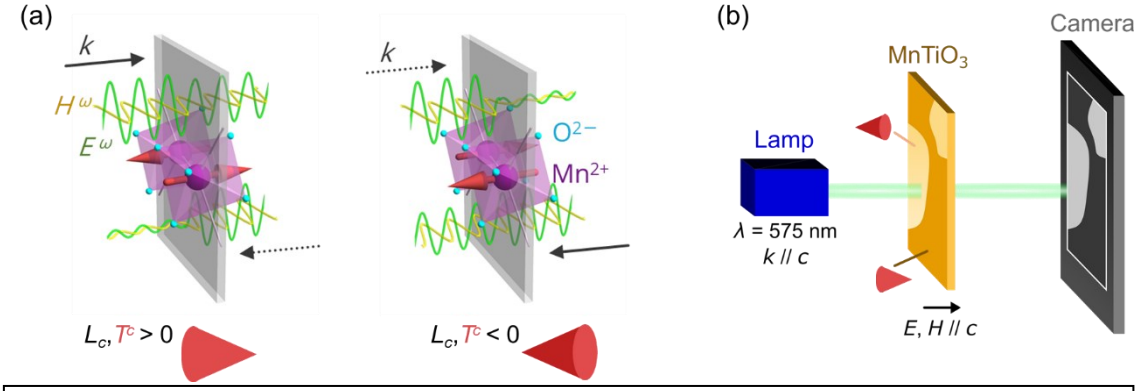

Figure 2: (a) Magnetochiral dichroism in $MnTiO_3$. (b) Visualization of ferrotoroidic domain pattern based on magnetochiral dichroism.

3.2 Ferrotoroidic domain imaging based on the nonlinear optical effect

Optical second harmonic generation (SHG), which is one of the second order nonlinear optical effect, is active when the system has no space inversion symmetry. This phenomenon can be described by using nonlinear susceptibility tensor χ_{ijk} as,

$$P_i(2\omega) = \varepsilon_0 \sum_{j,k} \chi_{ijk} E_j(\omega) E_k(\omega) \tag{2}$$

The polarization $P(2\omega)$ induced by electric field $E(\omega)$ of incident light becomes a source term and emit a frequency-doubled light beam. χ_{ijk} reflects the symmetry of the materials. Therefore, SHG is a sensitive probe of materials' symmetries. Magnetic toroidal moment $\boldsymbol{T}$, the target of this study, breaks space inversion symmetry. Thus, SHG can detect it directly only under T_N. Furthermore, the sign of χ_{ijk} depends on the direction of $\boldsymbol{T}$, as expressed by the relation $\chi_{ijk}(-\boldsymbol{T}) = -\chi_{ijk}(+\boldsymbol{T})$.

In the above discussion, we consider only electric-dipole transition. When we consider magnetic-dipole transition, SHG can emerge even in the system with space inversion symmetry. The SHG term whose polarization $P(2\omega)$ is induced by both electric field $E(\omega)$ and magnetic field $H(\omega)$ of incident light appears as

$$P_i(2\omega) = \varepsilon_0 \sum_{j,k} \chi_{ijk} E_j(\omega) H_k(\omega) \tag{3}$$

This SHG term comes from the crystal structure with space inversion symmetry and nonzero in all temperature range.

Replacing nonlinear susceptibility in equations (2) and (3) with χ^T and χ^{cr}, respectively, the SHG intensity under T_N is expressed as [see also Fig. 3(a)]

$$I(2\omega) \propto |\chi^{\mathrm{cr}} + \chi^T(\pm\boldsymbol{T})|^2 I(\omega)^2 = |\chi^{\mathrm{cr}} \pm \chi^T|^2 I(\omega)^2 \tag{4}$$

Equation (4) means that the interference between SHGs from crystal structure and magnetic toroidal

moment creates a contrast in the SHG intensity, and we can visualize the ferrotoroidic domain pattern by SHG as figure 3(b). In order to observe the domain structure near the surface, we measured SHG signal in transmission configuration with SHG wavelength of 400 nm (incident light: 800 nm), which is in charge transfer transition region. Using this wavelength, we can visualize the domains within approximate 50 nm

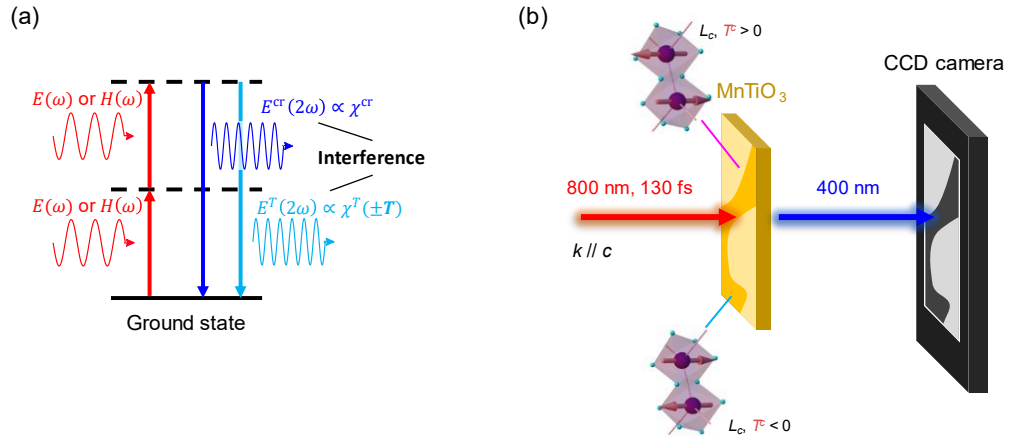

Figure 3: (a) Schematic image of SHG in $MnTiO_3$. (b) Visualization of ferrotoroidic domain pattern based on SHG.

from the surface.

4. Results and discussions

4.1 Visualization of ferrotoroidic domain pattern by MCHD

Figure 4 shows the ferrotoroidic domain pattern obtained by the MCHD-based imaging. Brighter and darker regions are observed in the right and left side in the circular field of view in Fig 4, respectively. Figure 4 is a difference image where the reference image taken at 65 K is subtracted from the original image taken at 55 K. The effects of inhomogeneous distribution of incident light intensity and the thickness of the sample do not appear in this difference image. Therefore, brighter and darker regions in Fig 4 are related with two states with ***T*** in opposite directions.

We can see several structural features of ferrotoroidic domain pattern from Fig 4. First, the fact that clear domain pattern is observed in the transmission configuration suggests that ferrotoroidic domain wall is oriented along the *c* axis. Second, three-fold symmetry in the underlying crystal structure is absent in the ferrotoroidic domain pattern. When the in-plane magnetic anisotropy is strong enough to confine the orientation of antiferromagnetic domain boundaries in the *c* plane, triangular or hexagonal patterns should arise in the ferrotoroidic domain pattern, considering the coupling between ***T*** and ***L***. Thus, absence of such pattern in ferrotoroidic domain pattern implies that in-plane magnetic anisotropy is not so strong to confine the in-plane orientations of multipole domain pattern. Finally, we can see that the typical size of the ferrotoroidic domains in $MnTiO_3$ is of 0.5-1 mm in width. This length scale is similar to that of antiferromagnetic domains in Cr_2O_3 with similar crystallographic and antiferromagnetic structures [5].

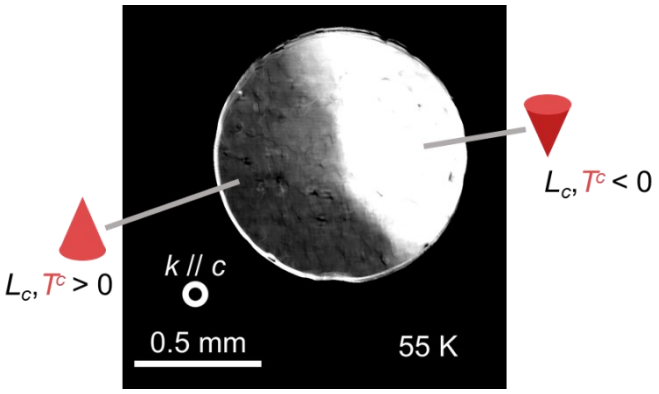

Figure 4: Ferrotoroidic domain pattern in $MnTiO_3$ at 55 K.

4.2 Visualization of ferrotoroidic domain pattern by SHG

Figure 5 shows the ferrotoroidic domain pattern obtained from SHG imaging. Figure 5 is composed of three images taken at 45 K. The polarization of incident light was right circular polarization and the left circular polarization component of SHG was detected. Below T_N, we obtained the image with clear contrast, while such contrasted patterns were not observed above T_N. Therefore, bright and dark regions in the contrasted image below T_N are related to ferrotoroidic domain with $\boldsymbol{T}$ in two different directions.

Figure 5 shows the domain pattern without three-fold rotational symmetry, like Fig. 4 does. However, the SHG image has a different information about domain size compared to one obtained from the MCHD image; while typical domain size is 0.5 to 1 mm in Fig. 5, there are some smaller domains with size of 0.1 mm or below 0.1 mm. Considering that by SHG-based imaging technique we observed the domains only near the surface, the result clearly suggests that ferrotoroidic domains with size of 0.1 mm is formed in $MnTiO_3$ near the surface. Furthermore, these small domains were not observed in the MCHD-based imaging, which observes averaged domain structures through the thickness. Thus, it is suggested that intricate ferrotoroidic domain wall with smaller length scale than 0.1 mm does not run along *c* axis.

In this SHG-based imaging experiment below T_N, we observed different ferrotoroidic domain patterns every time after the sample is warmed up above T_N and then cooled down below T_N. This behavior clarifies that there is no memory effect in the formation of ferrotoroidic domains in $MnTiO_3$.

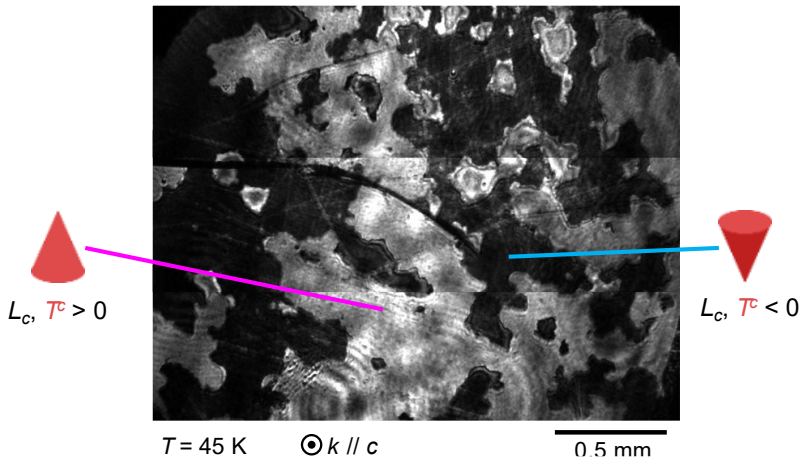

Figure 5: Ferrotoroidic domain pattern in $MnTiO_3$ at 45 K obtained from SHG imaging.

5. Summary

In this study, we performed imaging study of ferrotoroidic domain patterns in antiferromagnetic $MnTiO_3$ by linear and non-linear optical effects, respectively. The domain patterns were successfully visualized in both imaging experiments. In surface-sensitive SHG-based experiments, we observed intricate ferrotoroidic domain patterns with characteristic length scale of 0.1 mm or smaller, which was absent in the domain patterns obtained in bulk-sensitive MCHD-based imaging experiments.

At this stage, the relation between the intricate patterns at the surface of sample and the larger domain patterns in the bulk of the sample is not clear. Implementation of the two types of imaging experiments in the single optical setup would be useful to clarify this point.

6. Acknowledgement

We thank Prof. Taka-hisa Arima, Prof. Yusuke Tokunaga, Prof. Masakazu Matsubara, and Prof. Shingo Katsumoto for the approval of this research project. We thank MERIT for providing us the opportunity to present the results of this collaboration.

6. References

[1] M. -T. Suzuki *et al*., Phys. Rev. B **95**, 094406 (2017)

[2] N. A. Spaldin *et al*., J. Phys.: Condens. Matter **20**, 434203 (2008)

[3] S. -W. Cheong *et al*., npj Quantum Mater. **5**, 3 (2020)

[4] T. Sato *et al*., Phys. Rev. Lett. **124**, 217402 (2020).

[5] M. Fiebig *et al*., Appl. Phys. Lett. **66**, 2906 (1995).